Retinal Oxygenation and Oxygen Metabolism in Abyssinian Cats with a Hereditary Retinal Degeneration

Lissa Padnick-Silver,[1,2] *Jennifer J. Kang Derwent,*[1,3] *Elizabeth Giuliano,*[4] *Kristina Narfström,*[4,5] *and Robert A. Linsenmeier*[1,6]

Purpose. To investigate the effects of a hereditary retinal degeneration on retinal oxygenation and determine whether it is responsible for the severe attenuation of retinal circulation in hereditary photoreceptor degenerations.

Methods. Seven adult Abyssinian cats affected by hereditary retinal degeneration were studied. Oxygen microelectrodes were used to collect spatial profiles of retinal oxygenation in anesthetized animals. A one-dimensional model of oxygen diffusion was fitted to the data to quantify photoreceptor oxygen utilization (Qo_2).

Results. Photoreceptor Qo_2 progressively decreased until it reached zero in the end stage of the disease. Average inner retinal oxygen tension remained within normal limits at all disease stages, despite the observed progressive retinal vessel attenuation. Light affected photoreceptors normally, decreasing Qo_2 by ~50% at all stages of the disease.

Conclusions. Loss of photoreceptor metabolism allows choroidal oxygen to reach the inner retina, attenuating the retinal circulation in this animal model of retinitis pigmentosa (RP) and probably also in human RP. As the degeneration progresses, there is a strong relationship between changes in the a-wave of the ERG and changes in rod oxidative metabolism, indicating that these two functional measures change together. (*Invest Ophthalmol Vis Sci.* 2006;47:3683–3689) DOI:10.1167/iovs.05-1284

A progressive attenuation of the retinal circulation is observed with the progression of photoreceptor degenerations in both humans (retinitis pigmentosa; RP)[1] and in animals with hereditary retinal degenerative disease.[2–6] We hypothesized that the pronounced vasoconstriction results from decreased oxygen utilization by the outer retina after photoreceptor loss. Because less choroidal oxygen is used by the photoreceptors, it should reach the inner retina, where oxygen is known to cause constriction of retinal vessels.[7–9] This theory is supported by the lack of hypoxia in the inner retinas of RCS rats after photoreceptor loss.[10] Vessels do not simply constrict. Eventually they are lost in animals with photoreceptor degenerations.[2,5,6,11] This can be prevented by placing mice with a hereditary degeneration under conditions of reduced atmospheric oxygen for several days.[6] These studies suggest not only a physiological role of oxygen, but a trophic (or antitrophic) one as well.

In the present study, we further examined the hypothesis that oxygen from the choroid is responsible for attenuation of the retinal circulation, by characterizing changes in retinal oxygenation and oxidative metabolism during the progression of a feline hereditary retinal degeneration in a colony of Abyssinian cats.[3] The autosomal recessive genetic defect in this animal is not yet known, but it exhibits a slow rod–cone degeneration similar to human RP. Using measurements of intraretinal oxygen tension (Po_2) in these animals and our mathematical model of oxygen diffusion and utilization,[12] we were able to quantify photoreceptor oxygen consumption and examine retinal Po_2 in the different stages of the disease. Our results offer insight into the effects of photoreceptor loss on outer retinal metabolism and inner retinal oxygen autoregulation in hereditary photoreceptor degenerations. We were also able to compare two indices of retinal function in the same animals, the metabolic aspects presented herein, and the ERG.[13] A preliminary report of these results has been presented (Linsenmeier RA, et al. *IOVS* 2000;41:ARVO Abstract 4721).

Methods

Animals

Eight Abyssinian cats affected by a hereditary retinal degeneration were studied. These are the same cats in which an ERG study, reported in this issue, was also performed.[13] Figure 1 shows fundus photographs in each stage of the disease. Three cats were in the earliest stages of the disease (stage 1), two cats were in the middle stage (stage 2), two cats were in the late stage (stage 3), and one cat was in the final stage (stage 4). The stage of the disease was determined by ophthalmoscopic fundus evaluation, as described earlier.[3,13] The hematocrit from one stage 3 animal was low because of surgical complications and continued to decrease during the experiment. In this animal, the earlier choroidal Po_2 and the inner retinal Po_2, which were in the normal range, are included in the reported data, but oxygen consumption data and later choroidal Po_2 data from this animal were not used. Electrode problems prevented data collection in one stage 2 animal. Data from animals with retinal degeneration were compared to similar data obtained from normal cats.[14]

Experimental Preparation

All efforts were made to minimize the pain and discomfort of the animals and all procedures followed the guidelines of the ARVO Statement for the Use of Animals in Ophthalmic and Vision Research.

From the Departments of [1]Biomedical Engineering and [6]Neurobiology and Physiology, Northwestern University, Evanston, Illinois; the [2]Division of Ophthalmology, Evanston Northwestern Healthcare, Glenview, Illinois; the [3]Department of Biomedical Engineering and Pritzker Institute of Biomedical Science and Engineering, Illinois Institute of Technology, Chicago, Illinois; and the [4]Department of Medicine and Surgery, College of Veterinary Medicine, and the [5]Department of Ophthalmology, Mason Eye Institute, University of Missouri, Columbia, Missouri.

Supported by National Eye Institute Grants R01EY05034 (RAL) and T32 EY07128 (LP-S), The Foundation Fighting Blindness (KN), the Swedish Medical Research Council (14X-12209) (KN), and the National Cancer Institute (24XS028) (KN).

Submitted for publication September 28, 2005; revised February 27 and April 5, 2006; accepted June 6, 2006.

Disclosure: **L. Padnick-Silver**, None; **J.J. Kang Derwent**, None; **E. Giuliano**, None; **K. Narfström**, None; **R.A. Linsenmeier**, None

The publication costs of this article were defrayed in part by page charge payment. This article must therefore be marked "*advertisement*" in accordance with 18 U.S.C. §1734 solely to indicate this fact.

Corresponding author: Robert A. Linsenmeier, Biomedical Engineering Department, Northwestern University, 2145 Sheridan Road, Evanston, IL 60208-3107; r-linsenmeier@northwestern.edu.

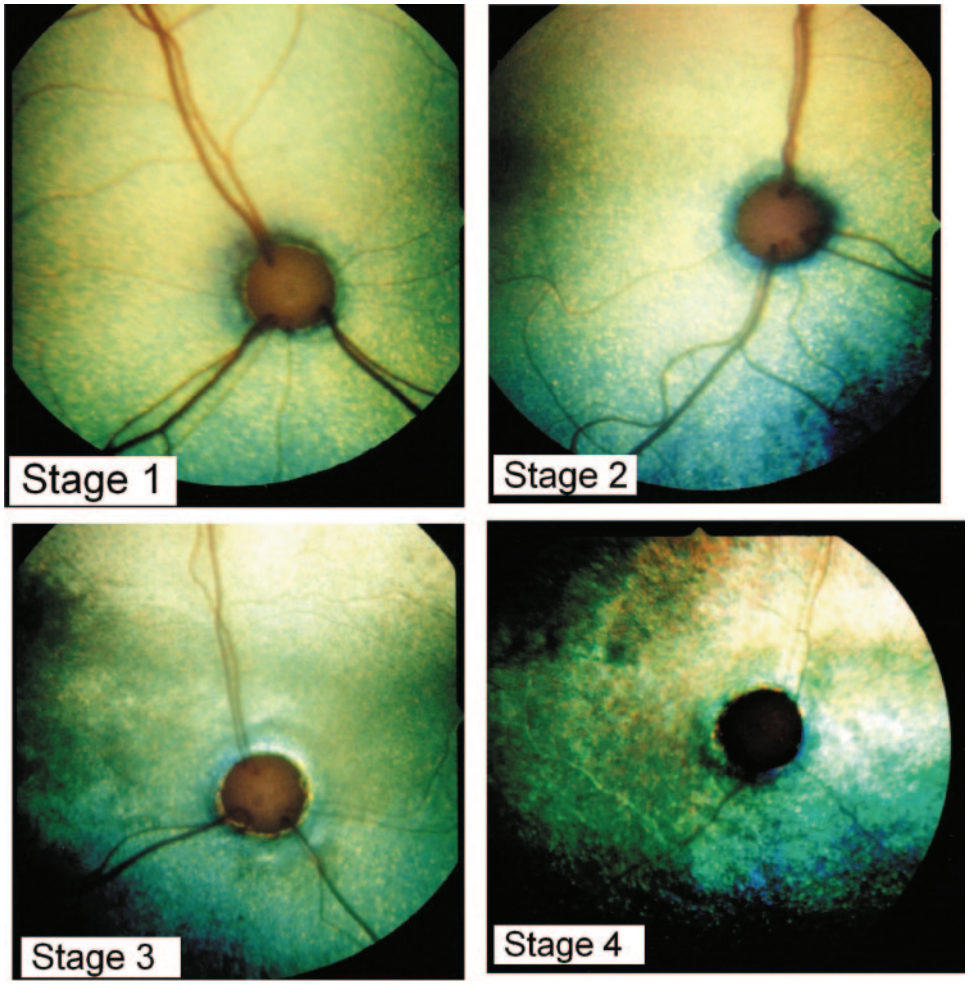

FIGURE 1. Fundus photographs of each of the four disease stages in Abyssinian cats. Stage 1 is characterized by a subtle tapetal fundus discoloration. In stage 2, the discoloration of the tapetum is more distinct and widespread, and peripheral vessels on the tapetal retina appear slightly attenuated. In stages 3 and 4, vessel attenuation is prominent, and the discoloration becomes darker and more mottled. Large areas of the tapetal fundus are hyperreflective.

Surgical and other setup procedures as well as histology are described in the companion paper.[13]

Electrodes

Intraretinal Po_2 was measured, as in previous experiments, with double-barreled polarographic oxygen microelectrodes.[15] One barrel recorded a current proportional to the oxygen tension of the tissue, whereas the other barrel, filled with 0.9% saline, recorded local intraretinal ERGs. An Ag/AgCl wire electrode in the vitreous recorded vitreal ERGs.

Data Collection

Po_2 spatial distributions (profiles) were recorded in regions surrounding the superior vessels, where fundus abnormalities were present, and in the central retina. The electrode penetrated the retina in 3-μm steps until the choroid was reached. A profile was then recorded while the electrode was withdrawn from the retina at a rate of 2 μm/s. ERGs were monitored during both penetration and withdrawal to assess the quality of the penetration and to determine the position of the electrode within the retina during recording of Po_2 profiles.

Modeling of Retinal Po_2

A three-layer diffusion model, developed and fully described previously,[12] was fitted to the outer, avascular portion of intraretinal Po_2 profiles. Briefly, the outer retina (photoreceptor layer) is divided into three anatomic layers: the outer segments (OS), the inner segments (IS), and the outer nuclear–outer plexiform layer (ONL-OPL). Because mitochondria are localized to the photoreceptor IS, oxygen is consumed only in this layer. The solution to the O_2 diffusion model (Po_2 versus distance) is derived from Fick's law of diffusion and is linear in nonconsuming regions (OS, ONL) and quadratic in the consuming region (IS). In this model we assume a steady state and that the diffusivity and solubility of oxygen, D and k, are constant throughout the retina. Figure 2A shows a simulated Po_2 profile and the parameters of the model.

Fick's Law as applied in this study is

$$\frac{d^2P}{dx^2} = \frac{Q}{Dk}. \quad (1)$$

Solving with the boundary conditions imposed by the model

$$P_1(x) = \alpha_1 x + \beta_1 \quad 0 \le x \le L_1, \quad (2)$$

$$P_2(x) = \frac{Q_2}{2Dk}x^2 + \alpha_2 x + \beta_2 \quad L_1 \le x \le L_2, \quad (3)$$

and

$$P_3(x) = \alpha_3 x + \beta_3 \quad L_2 \le x \le L, \quad (4)$$

where α_i and β_i are constants determined from the boundary conditions, P is the partial pressure of oxygen, L_1 is the position of the photoreceptor IS-OS boundary, L_2 is the position of the IS-ONL boundary, L is the position of the inner–outer retinal boundary, Q_2 is the

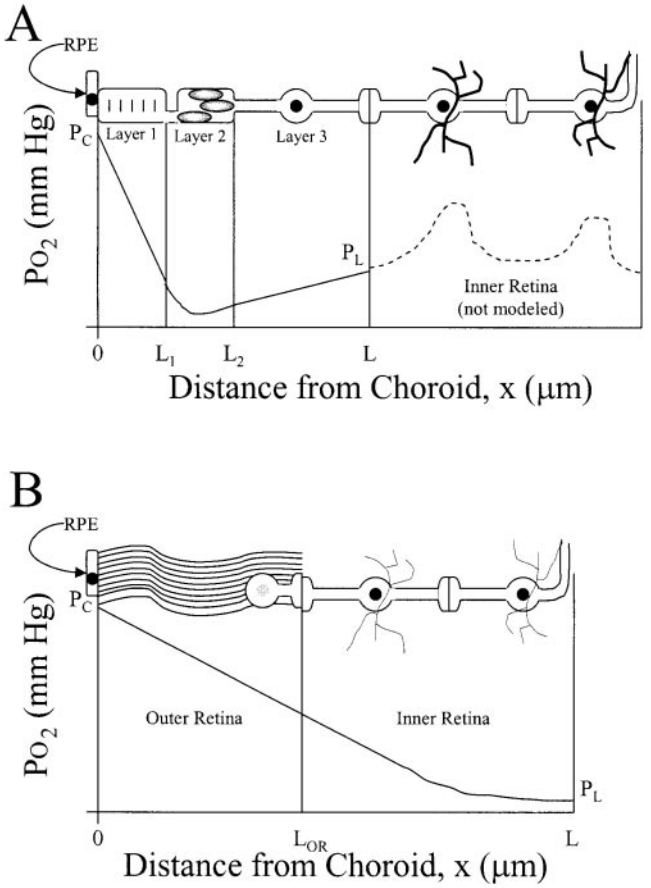

FIGURE 2. (**A**) Simulated data to show a normal retinal Po_2 profile and the three-layer diffusion model that describes outer retinal oxygenation. (**B**) Simulated data to show a retinal Po_2 profile and the two-layer diffusion model that describes the entire retina when the photoreceptors do not consume oxygen.

oxygen consumption of the IS layer, between L_1 and L_2, D is the diffusivity of oxygen through the retina, and k is the solubility of oxygen.

In this study, oxygen consumption is reported as outer retinal oxygen consumption (Q_{OR}), a weighted average of the three layers.

$$Q_{OR} = Q_2 \cdot \frac{L_2 - L_1}{L}. \quad (5)$$

The three-layer model could not be adequately fitted to many profiles from cats in stage 3 and 4 of the disease because of severe photoreceptor degeneration and therefore near-zero oxygen consumption. We normally assume that the outer retina is approximately 50% of the normal retinal thickness, but because the outer retinal layers thin late in the disease progression, this assumption was no longer valid. We therefore used a two-layer model where the boundary between the inner and outer retina was a modeled parameter. Layer 1 was the outer retina, and layer 2 was the inner retina. A schematic of the model with simulated data is shown in Figure 2B. The inner retina in normal cats is not described by our one-dimensional model because of the three-dimensional oxygen gradients created by the capillary network of the retinal circulation. In the late stages of this retinal degeneration, the severe decrease in retinal blood flow[16] allowed us to assume that the oxygen supply from the retinal circulation was negligible, which allowed inner retinal modeling. The solution to the general two-layer model is

$$P_1(x) = \frac{Q_1}{2Dk}x^2 + \alpha_1 x + \beta_1 \quad 0 \le x \le L_{OR} \quad (6)$$

and

$$P_2(x) = \frac{Q_2}{2Dk}x^2 + \alpha_2 x + \beta_2 \quad L_{OR} \le x \le L, \quad (7)$$

where L_{OR} is the boundary between the inner and outer retina, L is the vitreoretinal boundary, and α_i and β_i are constants dependent on the boundary conditions.

Assuming that $P_x = 0 = P_C$, $P_{x=L} = P_L$, $P_1 = P_2$ at $x = L_{OR}$, and that the oxygen gradient (first derivative) at $x = L_{OR}$ is equal for the two layers, α_i and, β_i are

$$\alpha_1 = \frac{Q_2 - Q_1}{Dk}L_{OR} + \alpha_2 \quad \beta_1 = P_C \quad (8)$$

and

$$\alpha_2 = \frac{Q_2}{2Dk}L + \frac{P_L - \beta_2}{L} \quad \beta_2 = \frac{Q_2 - Q_1}{2Dk}L_{OR}^2 + \beta_1. \quad (9)$$

After fitting all data that could not be adequately fitted with the usual three-layer model, we determined that oxygen consumption by the outer retina (layer 1), Q_{OR}, was not significantly different from zero. Therefore the profiles fit to the general two-layer model were refitted to a special two-layer model where consumption in layer 1, Q_1, was set to zero.

Fundus Photography

Fundus photographs were taken on 100 ASA color film with a fundus camera (Genesis; Kowa, Tokyo, Japan) set at the lowest flash intensity. A 1-log-unit neutral-density filter was inserted into the camera to reduce the flash intensity further.

Statistics

Selected parameters in Abyssinian cats were compared with those in normal cats with unpaired *t*-tests performed under the assumption that each oxygen profile gave an independent measurement of each parameter tested. This is recognized to be less satisfactory than treating each cat as independent, but was necessary because of the small number of cats with late-stage disease available.

RESULTS

Dark-Adapted Po_2 Profiles of the Outer Retina

Figure 3 shows examples of profiles recorded in each stage of the disease. Profiles recorded during dark-adaptation in stage 1 (Fig. 3B) were similar to those recorded from normal cats (Fig. 3A) on a gross level, however only 59% of profiles from stage 1 cats had the typical local minimum Po_2 in the outer retina. Even when a minimum was present, it was significantly higher in stage 1 cats (8.5 ± 4.4 mm Hg) than in normal animals (5.25 ± 5.12 mm Hg; $P = 0.026$). As the disease progressed, the outer retinal portion of the profile exhibited less curvature, a qualitative indicator of decreased Qo_2, and no local minimum existed in the outer retina in any profiles from cats in stages 2, 3, or 4 of the disease. This alone means that choroidal oxygen is reaching the inner retina.

Average choroidal Po_2 (P_C) was 55.7 ± 13.2 mm Hg in normal cats[14] ($n = 11$ cats, 46 profiles), 46.3 ± 8.8 mm Hg in stage 1 cats ($n = 3$ cats, 40 profiles), 50.9 ± 5.5 mm Hg in the stage 2 cat (9 profiles), 39.4 ± 3.7 mm Hg in stage 3 cats ($n = 2$ cats, 36 profiles), and 87.1 ± 9.5 mm Hg in the stage 4 cat (10

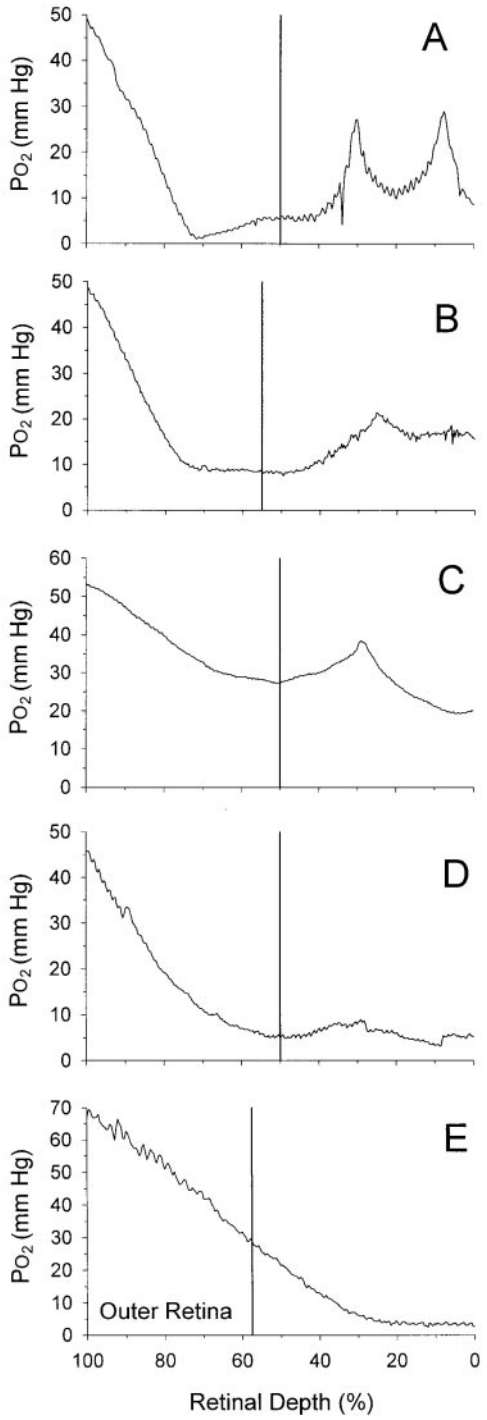

FIGURE 3. Spatial distributions of oxygen in a normal cat and in cats at each stage of the retinal degeneration. Each panel represents a single electrode withdrawal from the choroid (100% retinal depth) to the vitreous (0% retinal depth). *Vertical line:* border between inner and outer retina. Local maxima in oxygen in the inner retina indicate that the electrode was close to a retinal capillary. (**A**) Normal, (**B**) stage 1, (**C**) stage 2, (**D**) stage 3, (**E**) stage 4.

profiles). P_C in affected cats was significantly different from that observed in normal cats ($P < 0.05$; *t*-tests), but always in the range observed in the normal animals (30.3–83.5 mm Hg).

Fitting the outer retinal portion of Po_2 profiles to the diffusion model revealed that photoreceptor oxygen consumption (Q_{OR}) progressively decreased as the disease advanced (Fig. 4). Average Q_{OR} was 4.12 ± 2.14 mL $O_2 \cdot 100\ g^{-1} \cdot min^{-1}$ in normal cats (n = 11 cats, 46 profiles; Braun and Linsenmeier[14]), 2.62 ± 0.75 mL $O_2 \cdot 100\ g^{-1} \cdot min^{-1}$ in stage 1 cats (n = 3 cats, 35 profiles), 1.71 ± 0.60 mL $O_2 \cdot 100\ g^{-1} \cdot min^{-1}$ in the stage 2 cat (n = 7 profiles), 0.97 ± 0.46 mL $O_2 \cdot 100\ g^{-1} \cdot min^{-1}$ in the stage 3 cat (n = 13 profiles) and 0.00 mL $O_2 \cdot 100\ g^{-1} \cdot min^{-1}$ in the stage 4 cat (n = 8 profiles). The trend was striking and approximately linear.

Effect of Light on Outer Retinal Oxygen Consumption

Light adaptation caused a decrease in photoreceptor oxygen consumption by approximately 50% in all Abyssinian cats studied (with the exception of stage 4 where Q_{OR} was not different from zero). This result agrees with the 50% decrease also observed in normal cats.[12,15]

Inner Retinal Po_2

The distribution of inner retinal Po_2 appeared grossly normal in stage 1 cats, with the presence of local oxygen peaks corresponding to retinal capillaries (Fig. 3B). Average inner retinal Po_2 in stage 1 cats was 14.0 ± 7.1 mm Hg (n = 3 cats, 35 profiles) and was not significantly different from that in normal animals (15.2 ± 9.3 mm Hg, n = 46 profiles, 11 cats).

In stages 2 and 3, the average inner retinal Po_2 was 22.0 ± 4.0 mm Hg (7 profiles) and 8.5 ± 4.0 mm Hg (13 profiles), respectively. The Po_2 measured for stages 2 and 3 were significantly different from normal, but well within the normal range (1.0–41.2 mm Hg). Average inner retinal Po_2 was 21.5 ± 9.1 mm Hg in stage 4 (n = 8 profiles)—again, not significantly different from that in normal cats.

Of interest, the number of oxygen peaks in the inner retina decreased progressively, from 1.65 ± 0.63 per profile in normal animals to 0.13 ± 0.35 per profile in the stage 4 animal (Fig. 5). Regression analysis of these data indicated that the slope was significantly different from zero whether or not the normal animals were included (slope = −0.32 peaks/stage, $r^2 = 0.71$, $P = 2.1 \times 10^{-5}$, n = 17 cats including normal animals; slope = −0.30 peaks/stage, $r^2 = 0.68$, $P = 0.02$, n = 7 cats without normal animals). These results are consistent with the

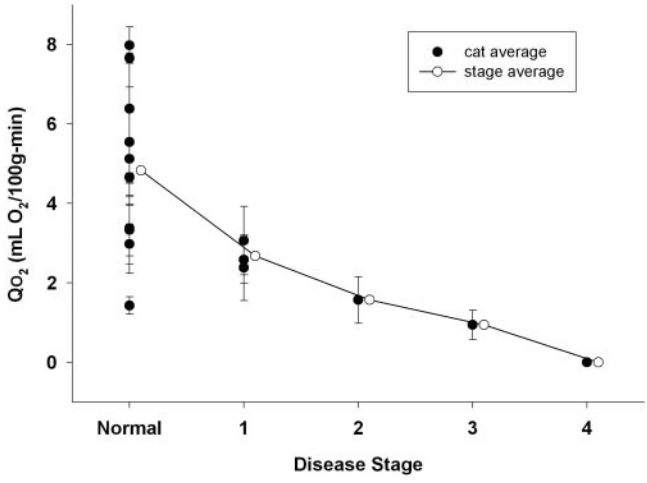

FIGURE 4. Photoreceptor oxygen consumption in normal cats and in cats at various stages of retinal degeneration. Data are averages for individual cats and the average outer retinal oxygen consumption for the stage shown on the *x*-axis. Error bars, SD. The line is a least-squares fit to the individual cat data, treating normal cats as stage zero: Q_{OR} = (−1.3139) · stage + 4.669; $R^2 = 0.4866$.

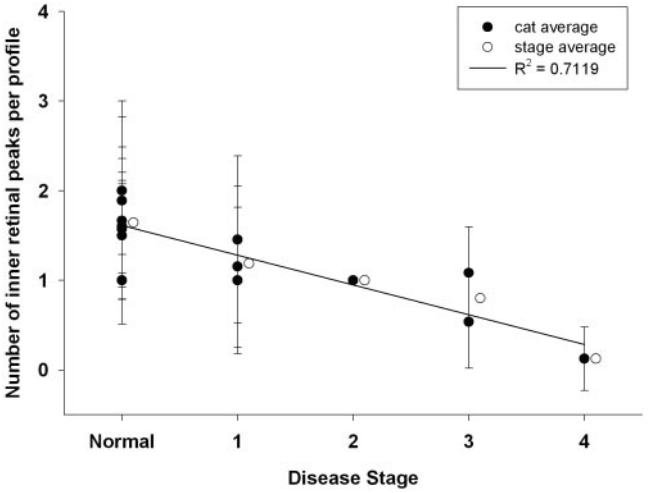

FIGURE 5. Number of local peaks in Po_2 per oxygen profile in the inner retina of cats at different disease stages. Data show the average number of peaks in one cat and the average for each stage. Error bar, SD. The *line* is a least-squares fit to the data from individual cats, treating normal cats as stage zero: Peaks = $(-0.3224) \cdot \text{stage} + 1.6128$; $R^2 = 0.7119$.

idea that retinal vessels are lost and that the choroid can maintain almost normal inner retinal Po_2.

In the stage 4 cat, we were able to model inner retinal oxygen consumption, as described in the Methods section, because of the drastic decrease in retinal blood flow in the final stages of the disease.[16] In this stage 4 cat, inner retinal oxygen consumption was slightly higher than that observed in normal cats (4.79 ± 1.32 mL $O_2 \cdot 100\ g^{-1} \cdot min^{-1}$; $n = 10$ profiles versus 3.77 ± 1.59 mL $O_2 \cdot 100\ g^{-1} \cdot min^{-1}$),[17] but the difference was not statistically significant.

DISCUSSION

Effects of Decreased Photoreceptor Metabolism on the Inner and Outer Retina

The oxygen distribution across the degenerating retina shifted from nearly normal in the early stages of the disease to markedly abnormal in the advanced stages. We were able to study only a few animals in these later stages, but the decrease in metabolism appeared to be progressive and steady. Incorporating more animals in the study would have allowed us to refine the shape of the function relating Q_{OR} to disease stage, which might become slightly more concave or convex than the linearity shown in Figure 4. In this study, the control animals were not Abyssinians, but domestic short-haired cats that were presumably genetically diverse. Previous work has shown that the ERG of such standard cats and unaffected Abyssinians is the same,[18] and we show in the accompanying paper[13] that their photoreceptor numbers are also the same. We have no reason to suspect that the metabolism of unaffected Abyssinians would be substantially different from the control animals we used.

Decreases in Q_{OR} altered the oxygen gradients, allowing oxygen from the choroidal circulation to reach the inner retina. This, in turn, allowed the inner retinal Po_2 to remain normal when the retinal circulation was attenuated. These points are emphasized by simulations of oxygen gradients, based on average parameters obtained from the diffusion model (Fig. 6). The simulations indicate that the normal oxygen gradient in the ONL, which usually brings oxygen from the retinal circulation to the photoreceptor IS, reverses in stage 2 of the disease. This gradient reversal demonstrates that choroidally derived oxygen, which is normally all used by the photoreceptors, can now reach the inner retina. From stage 2 forward, the choroid provides more and more oxygen to the inner retina. Because the central retina did not become substantially thinner until stage 4 in the cats used in the oxygen study, the distance from choroid to inner retina was taken to be the same in all but the stage 4 simulation. In stage 4, thinning of the retina contributed to increasing the transport to the inner retina beyond what would have been observed if the photoreceptors had been totally dysfunctional, but still present. Some thinning occurred, on average, in stage 3 (see Fig. 7H of Ref. 13), and so the simulation may slightly underestimate the effect of choroidal oxygen at this stage.

Another conclusion that is emphasized by Figure 6 is that, with the elevation of the minimum Po_2 well above zero, or loss of the minimum completely, the Po_2 at the choroid is not the limiting factor for metabolism, as it is in the normal retina.[15,19] Therefore, in retinas with degeneration, any variation of P_C between cats cannot explain the variation of Q_{OR} in the different disease stages.

The observation that vessels constrict severely in later stages of the disease provides one piece of information that oxygen autoregulatory capabilities remain largely intact throughout disease progression, even though the vessels are small. This argument is further strengthened by direct measurements of vascular reactivity to hypoxia and hyperoxia (Linsenmeier RA, et al. *IOVS* 2003;44:ARVO E-Abstract 543).

Our conclusions on the mechanism of vascular attenuation are similar to those in previous work. Noell[20] first suggested that vascular attenuation after loss of photoreceptors was dependent on oxygen. After destroying rods in monkey and cat retina with iodoacetic acid, Noell observed vasoattenuation essentially identical with that in RP. He reasoned that without photoreceptors, the metabolic demand of the retina would be lower, and so it would no longer need two circulations and would adapt. It made sense to him that the retinal rather than choroidal circulation would be lost, because retinal vessels were already known to be more responsive to metabolic factors, of which he mentioned high O_2 and low CO_2, than the choroidal vessels. Penn et al.[6] emphasized the importance of choroidal oxygen in the degeneration of retinal capillaries in a transgenic mouse retina, in which they found that systemic hypoxia for several days was able to prevent the loss of capil-

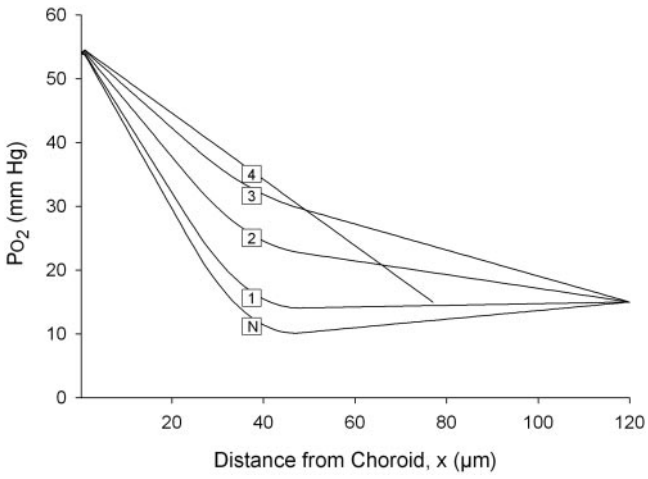

FIGURE 6. Simulations of oxygen profiles based on average parameters derived from the fits to data. Note the reversal of the oxygen gradient in the ONL in stage 2 of the disease. The thickness of the retina was the same in all stages except stage 4, where it was reduced, as shown.

laries. Yu et al.[10] made intraretinal oxygen measurements in the RCS rat retina and reached some of the same conclusions that we did about the flux of choroidal oxygen, but they did not report Qo_2 or the correlation with the ERG (see below). The thinning of the retina in the RCS rat appeared to proceed at about the same rate as changes in the oxygen gradients, whereas the percentage of change in thickness was smaller than the oxygen change in cats. Although there may be subtle differences among animal models, the feature of attenuation and loss of the retinal vasculature is common to all animal models of RP,[2–6] is prevalent in human RP[1] as well, and probably has fundamentally the same cause.

An alternate explanation for some of these data is that in the absence of photoreceptors, inner retinal metabolism decreases, and, because the retinal circulation is sensitive to metabolic demand, it shuts down, whether or not oxygen is coming from the choroid.[1] The fact that hypoxia preserves the retinal circulation in animals with photoreceptor degeneration[6] argues against this explanation and indicates that the inner retina still needs oxygen from some source. In addition, the present work provides the only direct evidence of any kind that the absence of photoreceptors does not change inner retinal metabolism to any great extent. This is somewhat tentative, because it is based on comparing inner retinal Qo_2 in one stage 4 cat to inner retinal Qo_2 in normal cats with retinal artery occlusion,[17] but it is based on multiple measurements in that one cat. It may initially be surprising that inner retinal metabolism would not be affected by the loss of photoreceptors, but consider what happens in the outer plexiform layer. Either all the photoreceptors will behave as if they are in darkness and release glutamate more of the time, or else they will become damaged and not release as much glutamate. In either case, they would produce less modulation of glutamate. In either case, because of the presence of parallel ON and OFF pathways, roughly half of the bipolar cells and other inner retinal neurons would experience steady depolarization, and the other half would experience steady hyperpolarization. The metabolic effects of more depolarization of some cells, which would be expected to increase their metabolism, and more hyperpolarization of other cells, which would decrease their metabolism, could well cancel out. It is more difficult to analyze the situation if and when the bipolar cells' glutamate receptors disappear.

Implications for Treatment

The loss of the retinal circulation will become a significant issue if photoreceptors or retinal progenitor cells can be restored to the retina of RP patients[21–24] or if the photoreceptors become functional via a gene transfer approach,[25–27] or if a prosthetic device is placed underneath the retina.[28,29] Natural photoreceptors would need oxygen again and therefore rob the inner retina of oxygen. Subretinal devices, no matter how permeable to oxygen, would increase the separation between the inner retina and the choroid. Even 100 μm would impair the delivery of oxygen to the inner retina.[19] It is unknown whether the retinal circulation could regrow after transgenic therapy or in the presence of a device, but the experience in all other diseases is that when new blood vessels grow in the adult retina, they are abnormal.

Mechanisms of Photoreceptor Loss

Stone et al.[30] and Walsh et al.[31] have shown that hyperoxia can be toxic to adult photoreceptors. Because the choroid does not regulate in response to oxygen levels,[32–34] as the photoreceptor outer segments become progressively less organized and use less oxygen, relative hyperoxia becomes progressively more severe. It may be that the initial photoreceptor defect would not lead to complete cell death in all types of RP if permanent hyperoxia did not result. Further, hyperoxia may play some role in killing cones. The prevalent hypotheses for why cones die in a disease where the rods are affected are (1) that rods produce a trophic substance that is needed by cones, or (2) that rods produce some toxic substance when they die.[35] The latter hypothesis is considered to be less likely because second-order neurons are preserved for a long time. There is direct support for a trophic factor from rods that protects cones,[36,37] but another factor in cone death could be increasing relative hyperoxia in a population of cells that is used to a low Po_2 environment.

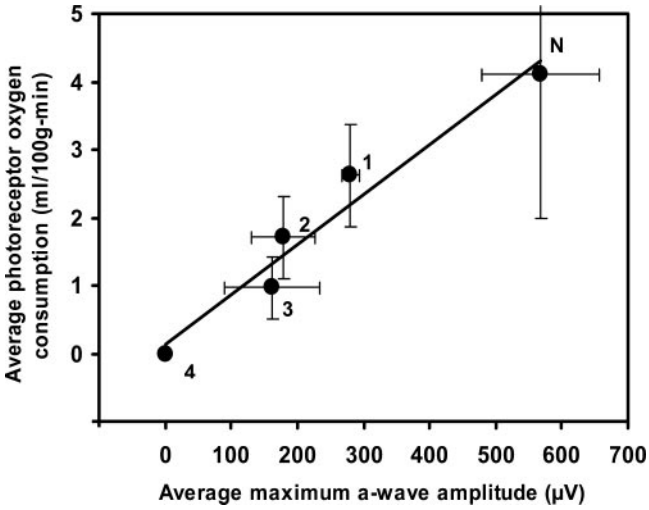

Figure 7. Correlation between photoreceptor oxygen consumption and the maximum amplitude of the a-wave (from Kang Derwent et al.[13]). *Symbols* show mean and standard deviations for all data in normal animals and at each stage of the disease. The regression line ($r^2 = 0.96$) is given by Qo_2 (mL $O_2 \cdot 100\ g^{-1} \cdot min^{-1}$) = (0.0073) · A-wave amplitude (μV) + 0.1397.

Correlating the ERG and Photoreceptor Metabolism

Figure 7 shows that photoreceptor Qo_2 correlates strongly with the a-wave of the ERG, another functional measure of photoreceptor activity. The maximum amplitude of the a-wave[13] and photoreceptor oxygen consumption decline virtually at the same rate during the disease ($r^2 = 0.956$, $P = 0.004$). This suggests that both measures are declining in Abyssinian cats as a result of the same underlying event. A substantial part of the functional decline is caused by loss of photoreceptors, but the functional measures, particularly the a-wave, tended to change more than the photoreceptor count in early stages.[13] Physiologically, one plausible scenario for the additional functional change is that if the outer segments are damaged, fewer of the light-dependent cation channels might be open in the dark. This would lead to a smaller influx of sodium, which would reduce the need for sodium pumping in the dark and thereby reduce oxidative metabolism. The presence of fewer cation channels would also hyperpolarize the dark resting potential, so that a smaller maximum excursion in membrane potential would be possible when the photoreceptor is illuminated, and that would reduce the maximum a-wave without changing transduction mechanisms or sensitivity.[13] The genetic event that underlies these physiological changes remains to be determined.

Acknowledgments

The authors thank Norbert Wangsa-Wirawan, Gulnur Birol, Ewa Budzynski, Christina Enroth-Cugell, and Yun Kim for assistance in the experiments and useful discussions.

References

1. Grunwald JE, Maguire AM, Dupont J. Retinal hemodynamics in retinitis pigmentosa. *Am J Ophthalmol*. 1996;122:502–508.
2. Gerstein DD, Dantzker DR. Retinal vascular changes in hereditary visual cell degeneration. *Arch Ophthalmol*. 1969;81:99–105.
3. Narfström K. Progressive retinal atrophy in the Abyssinian cat: clinical characteristics. *Invest Ophthalmol Vis Sci.* 1985;26:193–200.
4. Matthes MT, Bok D. Blood vascular abnormalities in animals with inherited retinal degeneration. In: La Vail MM, Hollyfield JG, Anderson RE, eds. *Retinal Degeneration: Experimental and Clinical Studies.* New York: Alan R. Liss; 1981:209–237.
5. Blanks JC, Johnson LV. Vascular atrophy of the retinal degenerative rd mouse. *J Comp Neurol*. 1986;254:543–553.
6. Penn JS, Li S, Naash MI. Ambient hypoxia reverses retinal vascular attenuation in a transgenic mouse model of autosomal dominant retinitis pigmentosa. *Invest Ophthalmol Vis Sci.* 2000;41:4007–4013.
7. Hickam JB, Frayser R. Studies of the retinal circulation in man: observation on vessel diameter, arteriovenous oxygen difference, and mean circulation time. *Circulation*. 1966;33:302–316.
8. Eperon G, Johnson M, David NJ. The effect of arterial Po_2 on relative retinal blood flow in monkeys. *Invest Ophthalmol Vis Sci.* 1975;14:342–52.
9. Riva CE, Grunwald JE, Sinclair SH. Laser Doppler velocimetry study of the effect of pure oxygen breathing on retinal blood flow. *Invest Ophthalmol Vis Sci.* 1983;24:47–51.
10. Yu D-Y, Cringle SJ, Su E-N, Yu PK. Intraretinal oxygen levels before and after photoreceptor loss in the RCS rat. *Invest Ophthalmol Vis Sci.* 2000;41:3999–4006.
11. Dantzker DR, Gerstein DD. Retinal vascular changes following toxic effects on visual cells and pigment epithelium. *Arch Ophthalmol*. 1969;81:106–114.
12. Haugh LM, Linsenmeier RA, Goldstick TK. Mathematical models of the spatial distribution of retinal oxygen tension and consumption, including changes upon illumination. *Ann Biomed Eng*. 1990;18:19–36.
13. Kang Derwent JJ, Padnick-Silver L. McRipley M, Giuliano E, Linsenmeier RA, Narfström K. The electroretinogram components in Abyssinian cats with hereditary retinal degeneration. *Invest Ophthalmol Vis Sci.* 2006;47;3673–3682.
14. Braun RD, Linsenmeier RA. Retinal oxygen tension and the electroretinogram during arterial occlusion in the cat. *Invest Ophthalmol Vis Sci.* 1995;36:523–541.
15. Linsenmeier RA, Braun RD. Oxygen distribution and consumption in the cat retina during normoxia and hypoxemia. *J Gen Physiol*. 1992;99:177–197.
16. Nilsson SFE, Maepea O, Alm A, Narfström K. Ocular blood flow and retinal metabolism in Abyssinian cats with hereditary retinal degeneration. *Invest Ophthalmol Vis Sci.* 2001;42:1038–1044.
17. Braun RD, Linsenmeier RA, Goldstick TK. Oxygen consumption in the inner and outer retina of the cat. *Invest Ophthalmol Vis Sci.* 1995;36:542–554.
18. Narfström, KL, Nilsson, SE, Andersson, BE. Progressive retinal atrophy in the Abyssinian cat: studies of the DC-recorded electroretinogram and the standing potential of the eye. *Br J Ophthalmol*. 1985;69:618–623.
19. Linsenmeier RA, Padnick-Silver L. Metabolic dependence of photoreceptors on the choroid in the normal and detached retina. *Invest Ophthalmol Vis Sci.* 2000;41:3117–3123.
20. Noell WK. Studies on the electrophysiology and metabolism of the retina. USAF Report No. 21-12-1-0004. 1953;122:104–106.
21. Humayun MS, de Juan E Jr, del Cerro M, et al. Human neural retinal transplantation. *Invest Ophthalmol Vis Sci.* 2000;41:3100–3106.
22. Lund RD, Kwan AS, Keegan DJ, Sauve Y, Coffey PJ, Lawrence JM. Cell transplantation as a treatment for retinal disease. *Prog Retin Eye Res*. 2001;20:415–449.
23. Sagdullaev BT, Aramant RB, Seiler MJ, Woch G, McCall MA. Retinal transplantation-induced recovery of retinotectal visual function in a rodent model of retinitis pigmentosa. *Invest Ophthalmol Vis Sci.* 2003;44:1686–1695.
24. Qui G, Seiler MJ, Mui C, et al. Photoreceptor differentiation and integration of retinal progenitor cells transplanted into transgenic rats. *Exp Eye Res.* 2005;80:515–525.
25. Acland GM, Aguirre GD, Ray J, et al. Gene therapy restores vision in a canine model of childhood blindness. *Nat Genet*. 2001;28:92–95.
26. Narfström K, Katz ML, Bragadottir R, et al. Functional and structural recovery of the retina after gene therapy in the PE65 mutation dog. *Invest Ophthalmol Vis Sci.* 2003;44:1663–1672.
27. Narfström K, Vaegan, Katz M, Bragadottir R, Rakoczy EP, Seeliger M. Assessment of structure and function over a 3-year period after gene transfer in RPE65$^{-/-}$ dogs. *Doc Ophthalmol.* 2005;111:39–48.
28. Chow AY, Pardue MT, Chow VY, et al. Implantation of semiconductor-based photodiodes into the cat subretinal space. *IEEE Trans Rehab Eng*. 2001;9:86–95.
29. Zrenner E. Will retinal implants restore vision? *Science*. 2002;295:1022–1025.
30. Stone J, Maslim J, Valter-Kocsi K, et al. Mechanisms of photoreceptor death and survival in mammalian retina. *Prog Retin Eye Res*. 1999;18:689–735.
31. Walsh N, Bravo-Nuevo A, Geller S, Stone J. Resistance of photoreceptors in the C57BL/6-c2J, C57BL/6J, and BALB/cJ mouse strains to oxygen stress: evidence of an oxygen phenotype. *Curr Eye Res*. 2004;29:441–447.
32. Friedman E, Chandra SR. Choroidal blood flow. 3. Effects of oxygen and carbon dioxide. *Arch Ophthalmol*. 1972;87:70–77.
33. Milley R, Rosenberg AA, Jones D Jr. Retinal and choroidal blood flows in hypoxic and hypercapnic newborn lambs. *Pediatr Res*. 1984;18:410–414.
34. Bill A, Nilsson SF. Control of ocular blood flow. *J Cardiovasc Pharmacol*. 1985;7(suppl 3):S96–S102.
35. Hicks D, Sahel J. The implications of rod-dependent cone survival for basic and clinical research. *Invest Ophthalmol Vis Sci.* 1999;40:3071–3074.
36. Mohand-Said S, Hicks D, Dreyfus H, Sahel JA. Selective transplantation of rods delays cone loss in a Retinitis Pigmentosa model. *Arch Ophthalmol*. 2000;118:807–811.
37. Leveillard T, Mohand-Said S, Lorentz O, et al. Identification and characterization of rod-derived cone viability factor. *Nat Genet*. 2004;36:755–759.